Title: Elevated Lactate in Acute Myeloid Leukemia Bone Marrow Microenvironment Dysfunction, with a Dual Role of GPR81 in Macrophage Polarization and Leukemia Cell Growth

Authors and Affiliations: Celia A. Soto[1,2,3], Maggie L. Lesch[2,4], Azmeer Sharipol[2,3,5], Amal Khan[2,3,4], Xenia L. Schafer[6], Michael W. Becker[2,7], Joshua C. Munger[4,6], Benjamin J. Frisch[1,2,3,5]

[1]Department of Pathology, University of Rochester School of Medicine, Rochester, NY, USA
[2]Wilmot Cancer Institute, University of Rochester Medical Center, Rochester, NY, USA
[3]Center for Musculoskeletal Research, University of Rochester Medical Center, Rochester, NY, USA
[4]Department of Microbiology and Immunology, University of Rochester School of Medicine, Rochester, NY, USA
[5]Department of Biomedical Engineering, University of Rochester School of Medicine, Rochester, NY, USA
[6]Department of Biochemistry and Biophysics, University of Rochester School of Medicine, Rochester, NY, USA
[7]Department of Medicine, University of Rochester School of Medicine, Rochester, NY, USA

Authors' Contributions: C. A. Soto: Conceptualization, experiments, data analysis, methodology, writing, and editing. **M. L. Lesch, A. Sharipol, and A. Khan:** assisted in experiments. **X. L. Schafer:** assisted with LC/MS-MS training and analysis. **M. W. Becker:** human samples and conceptualization. **J. C. Munger:** Conceptualization, methodology, and data analysis. **B. J. Frisch:** Conceptualization, data analysis, methodology, reviewing/editing, and oversight of the project.

Running Head: Lactate-GPR81 Signaling in AML Progression

Keywords: Acute Myeloid Leukemia (AML), bone marrow microenvironment, hematopoiesis, lactate, macrophages

Corresponding Author: Benjamin J. Frisch, Ph.D., University of Rochester Medical Center, School of Medicine and Dentistry. 601 Elmwood Avenue, Box 704, Rochester, NY, 14642. 1-(585)-275-5082, Benjamin_Frisch2@urmc.rochester.edu

Data Availability Statement: The metabolomics and RNAseq datasets generated and analyzed during the study, and any other raw data, were made available from the corresponding author upon request.

Funding: Financial support from the Wilmot Cancer Institute Research Development Funding Program Pilot Award to Dr. Frisch and Dr. Munger, and from a National Research Service Award (NRSA) Institutional Research Training Grant (T32) from the NIH to Celia Soto through the Rochester Musculoskeletal (ROCMSK) Training Program at the University of Rochester Center for Musculoskeletal Research (CMSR).

Total Number of Figures and Tables: 6 main figures, 6 supplementary figures, 2 tables, and 2 supplementary tables, supplementary methods, and 2 supplementary methods tables.

Acknowledgments: The human BM aspirate samples were obtained by Dr. Michael Becker, MD, and the bcCML model bacterial plasmids come from the lab of Dr. Laura Calvi, MD, of the Wilmot Cancer Institute. We thank Dr. Vadivel Ganapathy, Ph.D. at Texas Tech University for sending the *Gpr81*$^{-/-}$ mice. The RNA sequencing and analysis were performed by the Genomics Research Center at the University of Rochester Medical Center. We thank Dr. Helene McMurray, Ph.D., of the Cell Biology of Disease Program at the University of Rochester School of Medicine and Dentistry for insight on accessing and analyzing publicly available data from cancer patient databases. We thank Dr. Danielle Benoit, Ph.D., Dr. Roman Eliseev, MD, Ph.D., and Dr. Omar Ajiltawi, MD, as well as lab members from the labs of Dr. Laura Calvi, MD and Dr. Jane Liesveld, MD, Yuko Kawano, MD, PhD, Mark LaMere, and Mitra Azadniv, PhD, of the University of Rochester Medical Center for their feedback and assistance during the development of the project. This work was supported in part by the Wilmot Cancer Institute Research Development Funding Program Award to Dr. Frisch and Dr. Munger, Dr. Frisch's institutional start-up funding, and by a National Research Service Award (NRSA) Institutional Research Training Grant (T32) from the NIH to Celia Soto through the Rochester Musculoskeletal (ROCMSK) Training Program at the University of Rochester Center for Musculoskeletal Research (CMSR).

ABSTRACT

Interactions between acute myeloid leukemia (AML) and the hematopoietic bone marrow microenvironment (BMME) are critical to leukemia progression and chemoresistance. We measured elevated extracellular metabolites in the BMME of AML patients, including lactate. Lactate has been implicated in solid tumors for inducing suppressive tumor-associated macrophages, and correlates with poor prognosis. We describe a role of lactate in the polarization of leukemia-associated macrophages (LAMs), using a murine model of blast crisis chronic myelogenous leukemia (bcCML). Elevated lactate also diminished the function of hematopoietic progenitors and stromal support *in vitro*. Mice genetically lacking the lactate receptor GPR81 were used to demonstrate lactate-GPR81 signaling as a mechanism of both the polarization of LAMs and the direct support of leukemia cells. We report microenvironmental lactate as a critical driver of AML-induced BMME dysfunction and leukemic progression, thus identifying GPR81 as an exciting and novel therapeutic target for the treatment of this devastating disease.

INTRODUCTION

Acute myeloid leukemia (AML) is within the top ten cancer subtypes with the most numerous deaths per year in the U.S. [SEER, NIH], with a ~90% mortality rate at five years past diagnosis in the most affected age group of 65+ [1]. Cell-targeted chemotherapies initially reduce leukemic burden; however, there are various adverse effects on hematopoietic tissues, and relapse occurs in most patients [2, 3]. AML patients are often poor candidates for more effective stem cell transplantation due to comorbidities [4]. With approximately 20,000 new cases in the United States annually [SEER, NIH] and an increasing global incidence [5], there is a clear, unmet need for safe and effective treatments.

Current treatments for AML are often ineffective due, in part, to dysfunction of the bone marrow microenvironment (BMME). The BMME consists of all interactions among cells and extracellular molecules within the bone marrow (BM). AML is a heterogeneous hematologic malignancy initiated by genetic mutations in immature myeloid progenitor cells. Leukemic myeloid-like blasts undergo an uncontrolled proliferation (clonal hematopoiesis) and accumulate in the BM and other tissues [6]. Secondary to BMME aberrations are cytopenia and eventual fatal infection, hemorrhage, or BM failure [7, 8]. To date, the molecular mechanisms of

94 the interactions between AML and the BMME in disease pathophysiology have not been fully
95 explored.

96 Signaling within the BMME directs blood cell precursors to be produced from
97 hematopoietic stem cells (HSCs) [9]. When not circulating, HSCs reside at endosteal and
98 perivascular areas within the BM termed HSC "niches" where they receive signals from
99 specialized cells to remain quiescent, self-renew, or exit the niche to begin to differentiate into
100 hematopoietic progenitors [10, 11]. Multiple cell types have been implicated in the regulation of
101 HSCs including specialized subsets of mesenchymal stromal cells (MSCs) [12-14], osteoblasts
102 (OBs) [15-18], skeletal lineage cells [19], endothelial cells [20-22], macrophages [23], and T cells [24]. Niche
103 cells signal by cell-cell contact and secretion of numerous regulatory factors, including
104 extracellular cytokines and inflammatory molecules [13, 25-31]. Therefore, the BMME must maintain
105 cellular and extracellular composition for hematopoietic homeostasis. BMME alterations can
106 initiate or support leukemogenesis, and, reciprocally, leukemia results in an altered BMME [29,
107 32, 33]; the consequence is diminished production of blood and immune cell populations.
108 Furthermore, AML cells take refuge at the niche, leading to relapse when leukemia stem cell
109 (LSC) populations survive and repopulate after treatment [34, 35]. Therefore, a thorough
110 understanding of the microenvironment is needed to improve treatment.

111 Recent advances in the knowledge of the solid tumor microenvironment (TME) of
112 multiple cancer types have revealed the complexities of cancer progression, leading to
113 breakthrough therapeutic approaches such as immunotherapies. However, immunotherapies
114 have not yet been effective in clearing LSC populations in AML [36]. The TME has highly altered
115 levels of extracellular metabolites and cytokines that render immune cells ineffective while
116 supporting cancer cells [37-39]. Thus far, the contribution of the extracellular metabolic landscape
117 toward AML progression has not been well-defined. The altered extracellular metabolites in the
118 TME often are attributed to the amplified metabolic drive of cancer cells and the small area
119 between cells within the tumor architecture [40]. In contrast, the BMME has a less compact tumor
120 architecture, with ample vessel availability for nutrient and oxygen transfer throughout. Our
121 research aimed to determine if similar metabolic microenvironmental mechanisms of cancer
122 progression apply to leukemias.

123 A hallmark of cancer is the metabolic switch to constitutive aerobic glycolysis, known as
124 "the Warburg effect" [41], and leukemia cells are dependent on this type of metabolism for survival

125 [42]. As a by-product of glycolysis, lactate is secreted to the extracellular microenvironment [43].
126 Normally, lactate is converted back to pyruvate by lactate dehydrogenase (LDH) for further use
127 of pyruvate as a metabolic substrate [44]; however, 5-30-fold elevation of lactate levels have been
128 reported in solid tumors [45] and this elevation correlates with poor prognosis [46]. Lactate is
129 imported/exported cellularly through monocarboxylate transporters (MCT)-1 and -4 and can
130 signal through multiple pathways: as the extracellular ligand for the cell-surface G-protein-
131 coupled hydroxycarboxylic acid receptor 1 (GPR81/HCAR1), and intracellularly as metabolic
132 fuel or by activating transcription factor hypoxia-inducible factor-1 (HIF-1) [44, 47-49]. These
133 pathways primarily coordinate the axis between oxidative phosphorylation and glycolysis, and
134 shifts in metabolism can influence cell phenotype, for example, the activation phenotype of
135 macrophages [50]. Lactate-GPR81 signaling was found to reprogram glucometabolism in breast
136 cancer cells and directly contribute to the immune landscape in the TME [51]. Downstream of
137 GPR81 activation in cancer cells, pathways are upregulated for growth and survival, DNA repair
138 proteins, chemoresistance (ex. ABCB1 transporter), and MCT1/4 expression [52-54]. Moreover,
139 GPR81-lactate signaling has dual effects of inciting immune evasion by upregulating PD-L1 on
140 cancer cells while dysregulating antigen presentation on immune cells [55, 56].
141 Furthermore, immunosuppressive tumor-associated macrophages (TAMs) correlate with
142 poor prognosis in multiple cancer types, with lactate signaling implicated as a mechanism of
143 polarization [57-61]. In the BMME, macrophages are integral to the HSC niche during normal
144 hematopoiesis and stress [62, 63], and they interact with MSCs to coordinate the circulation of
145 HSCs [14]. While recent studies show alternatively activated leukemia-associated macrophages
146 (LAMs) and suggest their influence on AML progression [64, 65], little is known about the functions
147 of LAMs and the mechanisms by which they are polarized to this phenotype. Therefore, we
148 hypothesized that metabolite-related alterations to macrophages, MSCs, or OBs likely disrupt
149 hematopoietic support, contributing to the pathologic loss of hematopoiesis observed in AML
150 progression. We also aimed to determine if, similar to solid tumors, lactate contributes to both
151 an alternative macrophage phenotype and direct support for malignant cells.
152
153 **RESULTS**
154

155 **Extracellular Metabolite Levels are Elevated in Bone Marrow of AML Patients, Including**
156 **Lactate**
157 To profile the exometabolome of the AML bone marrow microenvironment (BMME), we
158 performed metabolomics on extracellular fluid from bone marrow (BM) biopsies of AML patients
159 at diagnosis, and healthy age- and sex-matched controls, by liquid chromatography coupled to
160 mass spectrometry (LC-MS/MS) (**Fig. 1A**) (See patient and control metrics in **Table S1**). This
161 revealed a global elevation of extracellular metabolites in the AML BMME (**Fig. 1B**), where
162 **Table 1** lists the metabolites with significantly altered levels (**Supplementary Fig. 1A**). To study
163 the consequences of elevated metabolites *in vivo*, we used a murine AML model of blast-crisis
164 chronic myelogenous leukemia (bcCML), where gene translocation products common to
165 myeloid leukemia (BCR-ABL) and (NUP98-HOXa9) are retrovirally inserted into hematopoietic
166 stem and progenitor cells (HSPCs/LSKs) to create malignant myeloid progenitor cells, that,
167 upon injection via tail vein, will engraft then accumulate rapidly in the BM, and irradiation is not
168 necessary to precondition the BM [66]. In this model, leukemic cells can be distinguished from
169 nonleukemic myeloid lineage cells, by the use of the leukemic genes conjugated to green
170 fluorescent protein (GFP) and yellow fluorescent protein (YFP) (**Fig. 1C**). The BMME at late-
171 stage bcCML (>50% leukemia cells in BM) also presented with elevated extracellular
172 metabolites (**Fig. 1D**), where **Table S2** lists the compounds with the most significantly altered
173 levels (identified in **Supplementary Fig. 1B**). The most highly altered metabolite in human AML
174 was lactate, with an extracellular lactate concentration approximately three times higher (**Fig.**
175 **1E**). The relative increase of lactate in the bcCML model was comparable to the human BMME
176 (**Fig. 1F** and **1G**), justifying the use of this model for our further studies on microenvironmental
177 lactate in AML pathology.
178
179 **Leukemia-Associated Macrophages are Alternatively Activated to a CD206^{hi},**
180 **Suppressive Phenotype**
181 We asked if elevated lactate has a role in the activation/polarization of local macrophages to a
182 pro-tumoral phenotype, as reported in solid tumors [57, 58, 60]. First, we determined whether
183 macrophages in the bcCML BM are alternatively activated. A survey of well-described activation
184 markers [CD38 and major histocompatibility complex class II (MHCII) = classic, pro-
185 inflammatory [67, 68]; macrophage mannose receptor (CD206) and early growth response protein

186 2 (EGR2) = alternative, suppressive/resolution-phase [69, 70]] was performed on BM macrophages
187 (Ly-6C$^-$, Ly-6G$^-$, CD45$^+$, F4-80$^+$) of bcCML mice (leukemia-associated macrophages (LAMs))
188 and non-leukemic (NL) controls (**Fig. 2A**) (See **Supplementary Methods Table SM2** for
189 markers and gating strategies). The software "Simplified Presentation of Incredibly Complex
190 Evaluations" (SPICE 6.1) (NIH) was used to identify an increased subset of LAMs that
191 overexpressed both CD206 and MHCII compared to NL macrophages (**Fig. 2B**). When
192 assessing these markers globally on LAMs, we observed an increase in the frequency of
193 CD206^{hi} macrophages (**Fig. 2C**) and expression level on the CD206$^+$ macrophages (**Fig. 2D**);
194 this was unique to non-leukemia-derived (GFP$^-$) macrophages and was elevated throughout the
195 disease course (**Supplementary Fig. 2A**). This suggests CD206 as a potential marker to
196 distinguish LAMs from myeloid leukemia cells in humans, of which there is not currently a good
197 marker for. The global frequency of MHCII was generally lower in LAMs, and CD38 and EGR2
198 were unchanged (**Supplementary Fig. 2B-D**). Splenic macrophages had a slightly higher
199 frequency of CD206$^+$ in bcCML, though the expression level on CD206$^+$ macrophages and the
200 frequency of CD206^{hi} macrophages were unchanged (**Supplementary Fig. 2E-I**). The increase
201 in CD206 expression was detectable on BM LAMs by an early-stage disease (7-10% leukemic
202 cells in the BM) (**Supplementary Fig. 2J** and **2K**).
203 To examine the functional phenotype of LAMs, transcriptional profiling was performed by
204 bulk RNA sequencing (RNAseq) of BM macrophages sorted from bcCML (LAMs) or NL controls.
205 The LAM transcriptome was distinctly different from NL macrophages (**Fig. 2E** and **2F**, and
206 **Supplementary Fig. 2L**). The top significantly downregulated pathways identified included
207 neutrophil interactions and cell cycle control (**Supplementary Fig. 2M**), while the top
208 upregulated pathways included interactions with immune and hematopoietic cells
209 (**Supplementary Fig. 2N**). This data indicates that LAMs are alternatively activated and may
210 contribute to the immune-privileged and dysregulated hematopoietic BMME observed in AML.
211 Proteome profiling detected several cytokines expressed by LAMs *in vitro* that were not
212 secreted by NL macrophages (**Fig. 2G** and **Table 2**). These cytokines have previously been
213 implicated in solid tumors as promoting tumor growth and metastasis (CXCL5, MMP3,
214 proprotein convertase 9) [71-73], regulating hematopoietic stem cell (HSC) development and
215 homing/mobilization (CXCL12)[74], and inducing a suppressive immune environment in the tumor

216 (CXCL10, CCL6) [75, 76], further suggesting a role of LAMs in the regulation of the BMME to
217 promote leukemic progression and suppress immune responses.
218 To isolate the contribution of lactate to the LAM phenotype, we treated bone marrow-
219 derived macrophages (BMDMs) *in vitro* with physiologically relevant levels of lactate: BM
220 extracellular lactate concentrations are likely higher *in vivo* than the measured concentrations
221 of ~2-5 mmol/L because AML patient BM biopsy samples are unavoidably diluted by some
222 peripheral blood upon collection. Also, we postulate that areas exist near AML cell-dense
223 pockets that are higher in lactate concentration, as the BM is known to be spatially
224 heterogeneous for concentrations of similar molecules, and pH [77]. Therefore, 5-15 mmol/L of
225 lactate was added for experiment treatments. As positive controls, we used lipopolysaccharide
226 (LPS) as proinflammatory stimuli [67], or interleukins (IL)-4 and -13 (IL-4, IL-13), well-described
227 Th2 cytokines produced in the resolution of inflammation regularly used as stimuli for alternative
228 macrophage activation [78-80]. We observed an additive effect of polarization to a $CD206^{hi}$
229 phenotype when lactate was combined with IL-4 and IL-13 (**Fig. 2H** and **2I**). This indicates that
230 lactate promotes polarization when some stimuli are present. The phenotype reversed after the
231 removal of stimuli for 48 hours (**Supplementary Fig. 2O** and **2P**), indicating that the activation
232 state is reversible. To assay for the function of $CD206^{hi}$ lactate-polarized BMDMs, we measured
233 transcript levels of Arginase 1 (Arg1): an enzyme involved in depleting L-arginase, the substrate
234 of inducible nitric oxide synthase (iNOS/Nos2), which mediates the cytotoxic production of nitric
235 oxide by classically-activated macrophages [69, 81]. Polarized BMDMs displayed increased *Arg1*
236 transcripts (**Fig. 2J**), while *iNOS* transcripts were not elevated (**Supplementary Fig. 2Q**). These
237 findings taken together suggest that macrophages in AML are likely suppressive, and that
238 excess lactate sensitizes macrophages to become alternatively activated.
239
240 **Elevated Lactate Negatively Regulates the Hematopoietic Bone Marrow**
241 **Microenvironment**
242 Within the unique cancer microenvironment of the bone marrow in AML, we must consider how
243 excess lactate may affect hematopoiesis. As we have previously reported [82], the murine model
244 of bcCML presented *in vivo* with an increase in the percentage of phenotypic hematopoietic
245 stem and progenitor cells (HSPCs), also known as LSK cells, and multipotent progenitors
246 (MPP): megakaryocyte-biased MPP2, myeloid-biased MPP3, and lymphoid-primed MPP4

247 (**Supplementary Fig. 3A-F,** see **Supplementary Methods Table SM2** for markers and gating
248 strategies). Also as previously reported, MSCs were expanded within the leukemic bone [29], a
249 key cell type for the maintenance of HSPCs; this was nonspecific to MSC subsets known to be
250 important to HSC adhesion and self-renewal at the niche: PDGFRα/CD51 (PααV) or
251 PDGFRα$^+$Sca-1$^+$ (PαS) MSCs (**Supplementary Fig. 3G-I**) [83-85]. Still, mature blood cell
252 populations are lost by late-stage bcCML [82], showing a dysfunction in progenitor cell
253 maintenance and/or differentiation.

254 To determine if lactate reduces the hematopoietic potential of HSPCs, colony-forming
255 unit cell (CFU-C) assays [39, 40] were performed: HSPCs/LSKs from healthy mice were
256 cocultured *in vitro* with a stromal monolayer and added "LSK" cytokines to promote the
257 maintenance of stemness, and were treated experimentally. They are then passaged to
258 methylcellulose-based MethoCult media (StemCell Technologies M3434) where they will grow
259 as colonies (CFU-Cs) if they retain hematopoietic potential. The stromal monolayer is grown
260 from the adherent cells from whole BM, and is composed of both a small percentage of MSCs
261 (>1%, like the percentage seen in the bone *in vivo*), and macrophages (**Supplementary Fig.
262 3J** and **3K**). As we have previously reported that aged macrophages can alter the colony-
263 forming potential of HSPCs [85], we tested the addition of LAMs to the cocultures compared to
264 macrophages from NL mice (**Fig. 3A**). The HSPCs showed reduced CFU-Cs when cocultured
265 with LAMs (**Fig. 3B**), suggesting a difference in hematopoietic maintenance signals. To
266 determine if lactate has direct effects on HSPCs, CFU-C assays were performed on HSPCs
267 alone (without a stromal monolayer). When treated with 10-15 mmol/L of lactate, HSPCs lost
268 colony-forming potential after 48 or 72 hours (**Fig. 3C**). We asked if stromal cells could maintain
269 HSPCs in the presence of lactate, CFU-C assays with lactate treatment were repeated on
270 cocultures of HSPCs with a stromal monolayer, however, cocultures treated with lactate for 72
271 hours also showed reduced CFU-Cs (**Fig. 3E and 3F**), suggesting that stromal cells do not
272 protect HSPCs from elevated lactate.

273 Next, we asked how excess lactate alters key stromal HSC niche cell types: MSCs and
274 their bone-forming progeny, osteoblasts (OBs). Stromal cultures that were differentiated to OBs
275 in the presence of increased lactate produced fewer pre-OB and OB colonies (**Fig. 3F-H**). This
276 is consistent with a loss of functional OBs and bone volume that we have previously reported
277 as a pathophysiology of AML [38]. Without differentiation, lactate also reduced MSC colony-

278 forming ability to fibroblasts (CFU-F), a measure of MSC self-renewal potential, [36, 37] and
279 decreased cell number after two weeks in culture (**Fig. 3I-K**). These results highlight multiple
280 damaging effects of elevated lactate on critical components of hematopoiesis in the BM.
281

282 **Lactate Signaling through GPR81 Contributes to the Suppressive Phenotype of**
283 **Leukemia-Associated Macrophages**

284 Lactate signals through multiple cellular pathways, therefore, we assessed which of these
285 pathways results in the observed lactate-mediated AML pathologies. To study this *in vivo*, we
286 considered the tools available: Genetic knockout of MCT1 is embryonically lethal [86], and while
287 MCT4 knockout mice are viable [87], MCT1 would be present which has a higher affinity for lactate
288 [88]. However, mice genetically lacking the lactate receptor GPR81 (*Gpr81*$^{-/-}$ or GPR81KO) grow
289 to healthy adulthood, produce blood cells at a normal ratio (**Supplementary Fig. 4A-F**), have a
290 similar weight and BM cellular density as wt mice (**Supplementary Fig. 4G-J**), and GPR81 has
291 been implicated in the regulation of the cancer microenvironment in solid tumors. Therefore, we
292 used GPR81KO mice to investigate the role of lactate-GPR81 signaling. First, wild type (wt)
293 bcCML was initiated in GPR81KO mice to eliminate GPR81 signaling from all non-leukemic BM
294 cells (**Fig. 4A**). The metabolomics of the BM extracellular fluid presented with elevated
295 metabolites at similar levels to bcCML in wt mice (**Supplementary Fig. 4K**), which confirmed
296 that this may be useful to study GPR81 signaling in the BMME during bcCML.

297 We reinvestigated the polarization of LAMs observed during bcCML when initiated in the
298 GPR81KO BMME. The increased frequency of macrophages observed in bcCML was partially
299 reversed in GPR81KO mice (**Fig. 4B**). The LAMs in the GPR81KO BMME expressed lower
300 CD206 levels, nearer to macrophages of healthy NL control mice (**Fig. 4C** and **4D**), and the
301 frequency of MHCII^{+} macrophages was higher (**Fig. 4E**). Other polarization markers were
302 increased or unchanged (**Supplementary Fig. 4L-P**). The GPR81KO mice displayed a similar
303 leukemic burden in the BM by the time of late-stage disease in wt mice, however, there was a
304 significant decrease in the frequency of leukemia cells in the peripheral blood and spleen
305 (**Supplementary Fig. 4Q-S**); this indicates a decrease in disease progression and/or a
306 reduction of peripheralization of leukemia cells.

307 Assays for BMDM polarization *in vitro* confirmed the contribution of GPR81 signaling as
308 a mechanism of LAM polarization; while they can be partially polarized, *Gpr81*$^{-/-}$ BMDMs did not

309 upregulate CD206 as highly as wt BMDMs (**Fig. 4F** and **4G**) and had a reduced range of *Arg1*
310 expression (**Fig. 4H**). To assay an additional signaling mechanism of lactate, we used
311 syrosingopine as a dual inhibitor of MCT1/4 and observed a contribution of MCTs to polarization
312 (**Supplementary Fig. 4T-V**), showing that other cell-internal signaling mechanisms of lactate
313 also promote the alternative activation phenotype. Next, we checked expression levels of lactate
314 signaling-related receptors in response to lactate treatment. When wt BMDMs were polarized,
315 we observed an upregulation of *Mct1* mRNA expression (**Supplementary Fig. 4W** and **4X**),
316 while there was not a significant increase in transcription of *Gpr81*, or *Mct4* (**Supplementary**
317 **Fig. 4Y** and **4Z**). However, we did not observe significant transcriptional changes in the
318 expression of *Gpr81*, *Mct1*, *Mct4*, or *iNOS* upon the polarization of GPR81KO BMDMs
319 compared to wt BMDMs (**Supplementary Fig. 4AA**). Therefore, this suggests that, in
320 macrophages, GPR81 sensing of lactate induces upregulation of MCT1 for lactate
321 import/export.
322
323 **GPR81-Lactate Signaling Has Modest Effects on the Hematopoietic BMME**
324 Next, we investigated which hematopoietic populations are impacted by GPR81 signaling. The
325 frequencies of hematopoietic progenitor, MSC, osteoblastic cell, and mature blood cell
326 populations were generally unchanged when bcCML was initiated in GPR81KO mice compared
327 to wt (**Fig. 5 A-I** and **Supplementary Fig. 5A**). This data, together with the fact that
328 nonleukemic, adult *Gpr81*$^{-/-}$ mice have appropriate ratios of mature blood cells, suggests that
329 GPR81 may be largely dispensable to hematopoiesis.
330 We assayed whether GPR81 signaling results in the observed lactate-mediated changes
331 to the colony-forming potential of HSPCs and MSCs. *Gpr81*$^{-/-}$ HSPCs showed a trend towards
332 a reversal of CFU-C loss at 5-10 mmol/L lactate with or without a stromal monolayer, but
333 potentiality still was lost by 15 mmol/L (**Fig. 5J** and **5K**). Also, lactate-treated *Gpr81*$^{-/-}$ MSCs still
334 displayed a loss of pre-OBs and fibroblastic colonies (**Fig. 5L** and **5M**). To note, we observed a
335 sex-dependent difference in CFU-F, where only MSCs from females were impacted by lactate
336 at 5-10 mmol/L (**Supplementary Fig. 5B** and **5C**). We then tested whether MCT1/4 signaling
337 is responsible for the losses at 15 mmol/L. First, treatment with syrosingopine at the 5 μM dose,
338 used for the macrophage polarization experiments, was lethal to the MSCs. Syrosingopine
339 treatments of 1 μM were not lethal, and caused a slight increase in CFU-F (**Supplemental Fig.**

340 **5D**). This demonstrates that MCT signaling is critical to MSC function; however, we note that
341 MCT inhibitors, if used therapeutically, may have effects on crucial MSC populations at lower
342 concentrations than to other cell types.
343 We assayed mRNA transcription levels of G*pr81* and *Mct1/4* by MSCs in response to
344 lactate treatment when GPR81 signaling is not present. *Gpr81*$^{-/-}$ MSCs had a lower upregulation
345 of *Mct4* than wt MSCs, while *Mct1* and *Gpr81* expression were similar to wt (**Supplementary**
346 **Fig. 5E-G**). Therefore, in MSCs, GPR81 may act as a lactate-sensor to regulate MCT-mediated
347 import/export of lactate; we hypothesize that this method of regulating intracellular lactate
348 concentration thereby influences the metabolic pathway primarily used by the cell (namely,
349 oxidative phosphorylation or glycolysis), which are known to influence the osteoblastic
350 differentiation fate of MSCs [89]. Altogether, these data show that GPR81 signaling has a modest
351 impact on hematopoietic cell types and MSCs, therefore, it may be possible to therapeutically
352 target lactate signaling in the BMME through this receptor with minimal consequences on
353 hematopoiesis; However, this will not protect the colony-forming potential of HSPCs and MSCs
354 from high lactate concentrations in bone.
355
356 **Lactate-GPR81 Signaling Drives Leukemia Cell Growth and Repopulation**
357 We hypothesized that BMME lactate also directly affects AML cells, as other cancer types have
358 found GPR81 signaling to promote growth, chemoresistance, and metastasis [52-54, 56]. To
359 determine if lactate enhances leukemia cell growth, *Gpr81*$^{-/-}$ bcCML cells were generated; these
360 were then used to initiate disease either in wt mice, or in GPR81KO mice (double-knockout
361 (DKO)) where GPR81 signaling is not present both on leukemic cells or in the BMME (**Fig. 6A**).
362 When GPR81KO bcCML cells were used, the leukemic burden was then largely reduced in the
363 BM, peripheral blood, and spleen of by the time point of late-stage disease in wt bcCML controls
364 (**Fig. 6B-D**). This may be attributed to the delayed rapid expansion of engrafted cells when
365 GPR81KO bcCML cells were used; leukemic burden was near zero at the time-point of early-
366 stage disease using wt bcCML cells (**Fig. 6E-H**). This led to an increased time to progression
367 to >50% leukemic cells in the BM in GPR81 DKO bcCML compared to wt (**Fig. 6I**). This data
368 suggests that leukemia cell GPR81 signaling impacts the rate of leukemia progression.
369 To verify the relevance of GPR81 signaling on human AML cells, analyses of publically
370 available databases were performed. First, 163 AML patient BM samples, from The Cancer

371 Genome Atlas (TCGA) Pan-Cancer Atlas database, were analyzed through cBioPortal for
372 Cancer Genomics (accessed at cbioportal.org) [90]. This dataset shows a rare subset of AML
373 patient samples with “altered”/high GPR81 (HCAR1) mRNA expression, and these patients
374 had a median survival time of 11 months less than those with “unaltered” HCAR1 (5.03 vs
375 16.08 months) (**Supplementary Fig. 6A**). No gene mutations or structural variants of HCAR1
376 were detected in AML subjects from TCGA datasets. This suggests that mutant HCAR1 is not
377 a contributor to AML transformation, but that dysregulation of HCAR1 expression may impact
378 prognosis. Analysis of another dataset of BM from 707 AML patients, BeatAML 2.0 (accessed
379 at vizome.org) [91], revealed that HCAR1 has a wider range of expression in tumor samples
380 than in healthy BM (**Supplementary Fig. 6B**), and correlates with disease state
381 (**Supplementary Fig. 6C**), where it is more dysregulated during initial diagnosis and relapse
382 than during remission. There are also trends towards higher HCAR1 expression when patients
383 had a lower survival time (**Supplementary Fig. 6D**). Together this expression data suggests
384 that GPR81/HCAR1 expression is more dysregulated in the BMME during AML, however, it is
385 not highly upregulated, and so suggests that the activity level of the receptor on the AML cells
386 may be more impactful than the change in expression level.
387 Finally, as residual leukemic stem cells (LSCs) after chemotherapy are the primary
388 reason for relapse in patients [34, 35], we determined the importance of GPR81 signaling to LSC
389 potential through serial passaging in methylcellulose-containing media. The *Gpr81*$^{-/-}$ bcCML
390 cells produced fewer colonies on average at P0 and P1 and lost repopulating capacity by P2-
391 P3, while wt bcCML cells continue to repopulate colonies to at least P7, suggesting that GPR81
392 is critical to LSC capacity (**Fig. 6J** and **6K**, and **Supplementary Fig 6E**). Together, these data
393 display the importance of GPR81 signaling to the rapid growth and repopulation of leukemia
394 cells.
395
396 **DISCUSSION**
397 In this research, we observe elevated levels of metabolites in the BMME during AML,
398 defining excess lactate as a critical driver of AML-induced BMME dysfunction and leukemia
399 progression. We identified lactate-GPR81 signaling as contributing to disease phenotypes of
400 leukemia-associated macrophages (LAMs) and AML cells. Therefore, our results highlight the

401 potential of GPR81 as a novel therapeutic target for both the leukemic suppression of the
402 immune system and AML self-repopulation.

403 We report a global elevation of extracellular metabolites in the BMME during AML (**Fig.**
404 **1**). An amino acid-rich leukemic microenvironment was observed, in contrast to a nutrient and
405 amino-acid-starved tumor microenvironment reported in most solid cancers [37]. This
406 distinguishes the leukemic BMME as a unique cancer microenvironment in need of further
407 investigation. It will be useful to study how leukemia cells and BM cells utilize these metabolites,
408 as they may act as signaling molecules or metabolic fuels. Notably, as lactate production is a
409 hallmark of cancer, findings on the mechanisms of lactate signaling to the immune system and
410 hematopoietic cells within the BMME are potentially applicable to multiple malignancies with
411 BM involvement, including additional types of leukemia as well as bone metastases of solid
412 tumors.

413 We demonstrate that GPR81 signaling promotes the alternative CD206^{hi} phenotype
414 observed in LAMs (**Fig. 2** and **Fig. 4**), which has been previously reported as a marker of
415 suppressive TAMs [92]. Additionally, this research identifies CD206 as a novel marker of LAMs
416 that is unique to non-leukemia-derived macrophages. AML cells display many myeloid and
417 macrophage markers, making them previously difficult to isolate from macrophages in the
418 human setting; therefore, CD206 may be useful to distinguish LAMs from myeloid leukemia
419 cells in patients. Furthermore, CD206 has been recently suggested as a prognostic factor for
420 AML [93], and is induced on monocytes cocultured with AML blasts [69]; these findings alongside
421 our research suggest that polarization of LAMs is due to AML cell secretion of lactate, and may
422 explain why this marker correlates with prognosis. It will be important to determine how GPR81
423 signaling interplays with additional signaling pathways to induce macrophage activation, such
424 as low pH, which has been indicated in the cooperation of lactic acid signaling with GM-CSF in
425 the polarization of breast cancer tumor-associated macrophages [94].

426 LAMs have an altered transcriptome; the upregulated transcripts, as well as the cytokine
427 release profile, suggest that they are functionally interacting with immune populations such as
428 T cells, and secreting cytokines that have been attributed to immunosuppression, HSC
429 development/mobilization, and tumor growth/metastasis [73, 74] (**Fig. 2** and **Supplementary Fig.**
430 **2**). This suggests a role of LAMs in the immune-privileged BMME known to occur in AML [69],
431 which gives benefit to leukemia progression and is partially responsible for the difficulties in

432 applying immunotherapies. More research is needed to determine if these cytokines influence
433 the BMME through similar mechanisms and cell types as has been found in solid tumors.
434 Furthermore, alternatively activated macrophages have been reported to induce
435 chemotaxis/differentiation of regulatory T cells (Tregs) which further the pro-tumor
436 microenvironment [76, 95, 96], and are inhibitory to T cells that would recognize tumor antigens [97].
437 For example, in a breast cancer model, GPR81 signaling in the microenvironment suppressed
438 $MHCII^{hi}$ immune cells and tumor-infiltrating T-cells, and GPR81 on tumor cells induced their
439 expression of PD-L1 inhibitory to antigen presentation [56]. Further research is needed to
440 determine if upregulated GPR81 signaling, directly and/or through altered antigen presentation
441 by macrophages, leads to such anti-lytic interactions between T cell populations and AML cells.
442 The repolarization of macrophages away from a suppressive phenotype by inhibition of GPR81
443 may have potential in combination with current chemotherapies, or to increase the efficacy of
444 immunotherapies, such as CAR-T cell therapy.

445 As AML progresses, cytopenia occurs as normal hematopoiesis is lost, secondary
446 to alterations to the BMME, thereby leading to fatal complications of the disease. This lactate-
447 high environment contributes to the loss of hematopoietic potential due to direct action on
448 HSPCs, as well as through alternative polarization of macrophages (**Fig. 3**). Lactate also
449 reduces hematopoietic support by critical HSC niche populations; stromal cells are impeded by
450 higher levels of lactate, leading to loss of growth and differentiation to osteoblasts (**Fig. 3**).
451 Others have found that lactate impedes osteogenic but not adipogenic differentiation of MSCs
452 [98], suggesting a possible role of lactate in the increased adipocytic BM that contributes to a pro-
453 tumoral BMME in AML [99].

454 Targeting lactate export through MCT inhibitors, and intracellular acidification, show
455 promising results as a target for the therapeutic inhibition of AML cells [100, 101]; however, the
456 implications for hematopoietic support populations within the BMME are unknown. The lethal
457 sensitivity that MSCs displayed experimentally to MCT inhibitors in this research raises concern
458 for targeting this pathway therapeutically. Furthermore, prior research in the field has attempted
459 to target various components of metabolic processes, such as lactate dehydrogenase (LDH),
460 for the treatment of AML cells but found that it also impaired normal hematopoiesis under stress
461 [42]. This highlights the need for a therapeutic option that can selectively diminish the function of
462 AML cells while having modest, or indeed, positive effects on the non-malignant hematopoietic

463 and BM support populations. The experimental removal of GPR81 described herein does not
464 negatively affect non-malignant populations, while partially rescuing the BMME (**Fig. 5**).
465 Relapse following chemotherapy is one of the greatest hurdles in treating AML. Our
466 results suggest that inhibition of GPR81 may be a viable strategy to prevent the repopulation of
467 AML cells following treatment; autocrine lactate signaling through GPR81 has been described
468 in solid tumors, and we find it as a critical receptor to bcCML cells for disease kinetics and
469 repopulating ability (**Fig. 6**). The signaling pathways downstream of GPR81 are numerous, and
470 multiple pathways have been investigated in cancer cell metabolism, DNA repair, and
471 chemoresistance [52-54]. Defining the signaling pathways downstream of GPR81 in AML and other
472 hematopoietic malignancies is promising for the identification of additional mechanisms to target
473 LSCs in the BM. Lastly, the development of a selective molecule to this receptor is strongly
474 supported by our findings, as there is currently no selective GPR81 antagonist available. In
475 conclusion, this research suggests that targeting GPR81 signaling in the BMME during AML
476 may be a selective and well-tolerated therapeutic option to prevent LSC repopulation and
477 rescue microenvironmental dysfunction.
478
479 **METHODS**
480
481 **Human Bone Marrow Extracellular Fluid Collection**
482 Deidentified bone marrow aspirates were collected from patients, and immediately centrifuged
483 to pellet cells. Following separation, the supernatant was stored at -80C until use.
484 **Murine Strains and Disease Models**
485 All murine experiments were performed using male and female wild type C57BL/6J mice or
486 *Gpr81*$^{-/-}$ mice on the same background. Experiments were performed using the following
487 murine model of AML: A previously established model of blast crisis chronic myelogenous
488 leukemia (bcCML) [29, 66, 82], an acutely progressing malignancy resulting in the accumulation of
489 myeloid blasts in the BM. For more information on murine strains and disease model
490 generation, see **Supplementary Methods**.
491
492 **Macrophage Polarization Experiments**

493 Treatment groups were serum-starved for 6 hours before treatment (DMEM, anti-anti, and M-
494 CSF without htFBS), and treatment conditions (100 ng/mL lipopolysaccharides (LPS) from E.
495 coli O55:B5 (Sigma L6529), or 5 ng/mL of recombinant murine interleukin (IL) -4 and -13 (IL-4,
496 IL-13) (ILs) (PeproTech 214-14, 210-13), were added to the serum-free media. To remove
497 cells for flow analysis, 0.25% trypsin-EDTA (Gibco 25200056) was added for 5 min then cell
498 scrapers were used to dislodge cells. Additional syrosingopine (Sigma SML 1908
499 resuspended in DMSO) treatments were done at 5 μM. To determine if this polarization is
500 reversible, we treated BMDMs with the polarization stimuli for 24 hours, then changed to fresh
501 media and cultured for one week. Stromal monolayer polarization was done similarly to
502 BMDM polarization, with 5 ng/mL of ILs and 10 mmol/L of lactate.
503
504 **Colony Forming Units (CFU-C) Assays for HSPC Potential**
505 To plate cells for CFU-Cs, all cells were collected from the wells by collecting the media with
506 non-adherent cells in a 15 mL conical tube, and then using 0.25% trypsin-EDTA on the
507 adherent cells for five minutes then flushing the wells with fresh MEM α and adding it to the
508 tube. Cells were pelleted by centrifugation for five minutes at 900 x g. Then, cells were
509 resuspended in 0.5 mL of MEM α. From here, both 1:20 and 1:100 dilutions were made in 2.5
510 mL of media in separate Eppendorf tubes. Then, 0.2 mL of these dilutions were resuspended
511 each in 2.5 mL aliquots of MethoCult (StemCell Technologies M3434) methylcellulose-
512 containing media and immediately plated in duplicates of 1.2 mL into 35mm x 10mm sterile
513 suspension culture dishes (Corning 430588). These were placed inside a sterile 150 mm x 25
514 mm dish (NEST 715001), with one open dish of sterile dH_20 in the center to retain humidity
515 and prevent drying of the cultures. These were incubated for 10-14 days (5% CO_2; 37C), then
516 colonies were counted using a microscope. For a description of experimental conditions see
517 **Supplementary Methods**.
518
519 **Leukemia Stem Cell (LSC) Assay**
520 Doubly-transfected (GFP^+, YFP^+) bcCML cells were sorted by FACS from the wt or *Gpr81*$^{-/-}$
521 bcCML primary spleen cell frozen stocks. Cells were plated at passage 0 (P0) in MethoCult as
522 described in CFU-C assays. After 10-14 days, four well-established colonies were picked,

523 resuspended in 200 µl of media, and replated at two dilutions. This continued until colonies
524 did not appear, or the seventh passage (P7) was reached.
525
526 **Rigor and Statistical Analysis**
527 All human and mouse samples were age- and sex-matched to control samples. Experiments
528 were replicated at least three times. Sample size analyses have been performed on all
529 preliminary data to ensure that subsequent repetitions were appropriately powered. Statistical
530 analyses were performed using GraphPad Prism 10 software.

References

1. Ferrara F, Schiffer CA. Acute myeloid leukaemia in adults. The Lancet. 2013;381(9865):484-495.
2. Crossnohere NL, Richardson DR, Reinhart C, et al. Side effects from acute myeloid leukemia treatment: results from a national survey. Current Medical Research and Opinion. 2019;35(11):1965-1970.
3. Thol F, Ganser A. Treatment of Relapsed Acute Myeloid Leukemia. Current Treatment Options in Oncology. 2020;21(8):66.
4. Gupta V, Tallman MS, Weisdorf DJ. Allogeneic hematopoietic cell transplantation for adults with acute myeloid leukemia: myths, controversies, and unknowns. Blood. 2011;117(8):2307-2318.
5. Yi M, Li A, Zhou L, Chu Q, Song Y, Wu K. The global burden and attributable risk factor analysis of acute myeloid leukemia in 195 countries and territories from 1990 to 2017: estimates based on the global burden of disease study 2017. Journal of Hematology & Oncology. 2020;13(1):72.
6. Döhner H, Weisdorf DJ, Bloomfield CD. Acute Myeloid Leukemia. New England Journal of Medicine. 2015;373(12):1136-1152.
7. Chang H-Y, Rodriguez V, Narboni G, Bodey GP, Luna MA, Freireich EJ. CAUSES OF DEATH IN ADULTS WITH ACUTE LEUKEMIA. Medicine. 1976;55(3):
8. Miraki-Moud F, Anjos-Afonso F, Hodby KA, et al. Acute myeloid leukemia does not deplete normal hematopoietic stem cells but induces cytopenias by impeding their differentiation. Proceedings of the National Academy of Sciences of the United States of America. 2013;110(33):13576-13581.
9. Till JE, McCulloch EA. A Direct Measurement of the Radiation Sensitivity of Normal Mouse Bone Marrow Cells. Radiation Research. 1961;14(2):213-222.
10. Schofield R. The relationship between the spleen colony-forming cell and the haemopoietic stem cell. Blood Cells. 1978;4(1-2):7-25.
11. Frisch BJ. The hematopoietic stem cell niche: What's so special about bone? Bone. 2019;119(8-12.

12. Asada N, Kunisaki Y, Pierce H, et al. Differential cytokine contributions of perivascular haematopoietic stem cell niches. Nature Cell Biology. 2017;19(3):214-223.
13. Greenbaum A, Hsu Y-MS, Day RB, et al. CXCL12 in early mesenchymal progenitors is required for haematopoietic stem-cell maintenance. Nature. 2013;495(7440):227-230.
14. Méndez-Ferrer S, Michurina TV, Ferraro F, et al. Mesenchymal and haematopoietic stem cells form a unique bone marrow niche. Nature. 2010;466(7308):829-834.
15. Calvi LM, Adams GB, Weibrecht KW, et al. Osteoblastic cells regulate the haematopoietic stem cell niche. Nature. 2003;425(6960):841-846.
16. Zhang J, Niu C, Ye L, et al. Identification of the haematopoietic stem cell niche and control of the niche size. Nature. 2003;425(6960):836-841.
17. Zhu J, Garrett R, Jung Y, et al. Osteoblasts support B-lymphocyte commitment and differentiation from hematopoietic stem cells. Blood. 2007;109(9):3706-3712.
18. Bowers M, Zhang B, Ho Y, Agarwal P, Chen C-C, Bhatia R. Osteoblast ablation reduces normal long-term hematopoietic stem cell self-renewal but accelerates leukemia development. Blood. 2015;125(17):2678-2688.
19. Green AC, Tjin G, Lee SC, et al. The characterization of distinct populations of murine skeletal cells that have different roles in B lymphopoiesis. Blood. 2021;
20. Kunisaki Y, Bruns I, Scheiermann C, et al. Arteriolar niches maintain haematopoietic stem cell quiescence. Nature. 2013;502(7473):637-643.
21. Acar M, Kocherlakota KS, Murphy MM, et al. Deep imaging of bone marrow shows non-dividing stem cells are mainly perisinusoidal. Nature. 2015;526(7571):126-130.
22. Fang S, Chen S, Nurmi H, et al. VEGF-C protects the integrity of the bone marrow perivascular niche in mice. Blood. 2020;136(16):1871-1883.
23. Chow A, Lucas D, Hidalgo A, et al. Bone marrow CD169+ macrophages promote the retention of hematopoietic stem and progenitor cells in the mesenchymal stem cell niche. Journal of Experimental Medicine. 2011;208(2):261-271.
24. Fujisaki J, Wu J, Carlson AL, et al. In vivo imaging of Treg cells providing immune privilege to the haematopoietic stem-cell niche. Nature. 2011;474(7350):216-219.
25. Sugiyama T, Kohara H, Noda M, Nagasawa T. Maintenance of the Hematopoietic Stem Cell Pool by CXCL12-CXCR4 Chemokine Signaling in Bone Marrow Stromal Cell Niches. Immunity. 2006;25(6):977-988.

26. Staversky RJ, Byun DK, Georger MA, et al. The Chemokine CCL3 Regulates Myeloid Differentiation and Hematopoietic Stem Cell Numbers. Sci Rep. 2018;8(1):14691.
27. Sitnicka E, Lin N, Priestley G, et al. The effect of thrombopoietin on the proliferation and differentiation of murine hematopoietic stem cells. Blood. 1996;87(12):4998-5005.
28. Arai F, Hirao A, Ohmura M, et al. Tie2/angiopoietin-1 signaling regulates hematopoietic stem cell quiescence in the bone marrow niche. Cell. 2004;118(2):149-161.
29. Frisch BJ, Ashton JM, Xing L, Becker MW, Jordan CT, Calvi LM. Functional inhibition of osteoblastic cells in an in vivo mouse model of myeloid leukemia. Blood. 2012;119(2):540-550.
30. Goncalves KA, Silberstein L, Li S, et al. Angiogenin Promotes Hematopoietic Regeneration by Dichotomously Regulating Quiescence of Stem and Progenitor Cells. Cell. 2016;166(4):894-906.
31. Winkler IG, Barbier V, Nowlan B, et al. Vascular niche E-selectin regulates hematopoietic stem cell dormancy, self renewal and chemoresistance. Nat Med. 2012;18(11):1651-1657.
32. Kode A, Manavalan JS, Mosialou I, et al. Leukaemogenesis induced by an activating β-catenin mutation in osteoblasts. Nature. 2014;506(7487):240-244.
33. Soto CA, Lo Celso C, Purton LE, Frisch BJ. From the niche to malignant hematopoiesis and back: reciprocal interactions between leukemia and the bone marrow microenvironment. JBMR Plus. 2021;5(10):e10516.
34. Ishikawa F, Yoshida S, Saito Y, et al. Chemotherapy-resistant human AML stem cells home to and engraft within the bone-marrow endosteal region. Nature Biotechnology. 2007;25(11):1315-1321.
35. Lapidot T, Sirard C, Vormoor J, et al. A cell initiating human acute myeloid leukaemia after transplantation into SCID mice. Nature. 1994;367(6464):645-648.
36. Isidori A, Cerchione C, Daver N, et al. Immunotherapy in Acute Myeloid Leukemia: Where We Stand. Frontiers in Oncology. 2021;11(
37. Bader JE, Voss K, Rathmell JC. Targeting Metabolism to Improve the Tumor Microenvironment for Cancer Immunotherapy. Molecular Cell. 2020;78(6):1019-1033.
38. Baltazar F, Afonso J, Costa M, Granja S. Lactate Beyond a Waste Metabolite: Metabolic Affairs and Signaling in Malignancy. Frontiers in Oncology. 2020;10(
39. Bejarano L, Jordão MJC, Joyce JA. Therapeutic Targeting of the Tumor Microenvironment. Cancer Discov. 2021;11(4):933-959.

40. Elia I, Haigis MC. Metabolites and the tumour microenvironment: from cellular mechanisms to systemic metabolism. Nature Metabolism. 2021;3(1):21-32.
41. Warburg O. On the origin of cancer cells. Science. 1956;123(3191):309-314.
42. Wang Y-H, Israelsen William J, Lee D, et al. Cell-State-Specific Metabolic Dependency in Hematopoiesis and Leukemogenesis. Cell. 2014;158(6):1309-1323.
43. Rogatzki MJ, Ferguson BS, Goodwin ML, Gladden LB. Lactate is always the end product of glycolysis. Frontiers in Neuroscience. 2015;9(
44. Brooks GA, Dubouchaud H, Brown M, Sicurello JP, Butz CE. Role of mitochondrial lactate dehydrogenase and lactate oxidation in the intracellular lactate shuttle. Proceedings of the National Academy of Sciences. 1999;96(3):1129-1134.
45. de la Cruz-López KG, Castro-Muñoz LJ, Reyes-Hernández DO, García-Carrancá A, Manzo-Merino J. Lactate in the Regulation of Tumor Microenvironment and Therapeutic Approaches. Frontiers in oncology. 2019;9(1143-1143.
46. Walenta S, Wetterling M, Lehrke M, et al. High lactate levels predict likelihood of metastases, tumor recurrence, and restricted patient survival in human cervical cancers. Cancer Res. 2000;60(4):916-921.
47. Ritzhaupt A, Wood IS, Ellis A, Hosie KB, Shirazi-Beechey SP. Identification and characterization of a monocarboxylate transporter (MCT1) in pig and human colon: its potential to transport l-lactate as well as butyrate. The Journal of Physiology. 1998;513(3):719-732.
48. DIMMER K-S, FRIEDRICH B, LANG F, DEITMER JW, BRÖER S. The low-affinity monocarboxylate transporter MCT4 is adapted to the export of lactate in highly glycolytic cells. Biochemical Journal. 2000;350(1):219-227.
49. De Saedeleer CJ, Copetti T, Porporato PE, Verrax J, Feron O, Sonveaux P. Lactate Activates HIF-1 in Oxidative but Not in Warburg-Phenotype Human Tumor Cells. PLOS ONE. 2012;7(10):e46571.
50. Viola A, Munari F, Sánchez-Rodríguez R, Scolaro T, Castegna A. The Metabolic Signature of Macrophage Responses. Frontiers in Immunology. 2019;10(
51. li X, Chen Y, Wang T, et al. GPR81-mediated reprogramming of glucose metabolism contributes to the immune landscape in breast cancer. Discover Oncology. 2023;14(1):140.
52. Ishihara S, Hata K, Hirose K, et al. The lactate sensor GPR81 regulates glycolysis and tumor growth of breast cancer. Scientific Reports. 2022;12(1):6261.

53. Roland CL, Arumugam T, Deng D, et al. Cell surface lactate receptor GPR81 is crucial for cancer cell survival. Cancer Res. 2014;74(18):5301-5310.
54. Wagner W, Kania KD, Blauz A, Ciszewski WM. The lactate receptor (HCAR1/GPR81) contributes to doxorubicin chemoresistance via abcb1 transporter up-regulation in human cervical cancer hela cells. Journal of Physiology and Pharmacology. 2017;68(4):555-564.
55. Feng J, Yang H, Zhang Y, et al. Tumor cell-derived lactate induces TAZ-dependent upregulation of PD-L1 through GPR81 in human lung cancer cells. Oncogene. 2017;36(42):5829-5839.
56. Brown TP, Bhattacharjee P, Ramachandran S, et al. The lactate receptor GPR81 promotes breast cancer growth via a paracrine mechanism involving antigen-presenting cells in the tumor microenvironment. Oncogene. 2020;39(16):3292-3304.
57. Gordon S, Martinez FO. Alternative Activation of Macrophages: Mechanism and Functions. Immunity. 2010;32(5):593-604.
58. Zhang QW, Liu L, Gong CY, et al. Prognostic significance of tumor-associated macrophages in solid tumor: a meta-analysis of the literature. PLoS One. 2012;7(12):e50946.
59. Zhang Q, He Y, Luo N, et al. Landscape and Dynamics of Single Immune Cells in Hepatocellular Carcinoma. Cell. 2019;179(4):829-845.e820.
60. Colegio OR, Chu N-Q, Szabo AL, et al. Functional polarization of tumour-associated macrophages by tumour-derived lactic acid. Nature. 2014;513(7519):559-563.
61. Mu X, Shi W, Xu Y, et al. Tumor-derived lactate induces M2 macrophage polarization via the activation of the ERK/STAT3 signaling pathway in breast cancer. Cell Cycle. 2018;17(4):428-438.
62. Winkler IG, Sims NA, Pettit AR, et al. Bone marrow macrophages maintain hematopoietic stem cell (HSC) niches and their depletion mobilizes HSCs. Blood. 2010;116(23):4815-4828.
63. Seyfried AN, Maloney JM, MacNamara KC. Macrophages Orchestrate Hematopoietic Programs and Regulate HSC Function During Inflammatory Stress. Frontiers in Immunology. 2020;11(
64. Al-Matary YS, Botezatu L, Opalka B, et al. Acute myeloid leukemia cells polarize macrophages towards a leukemia supporting state in a Growth factor independence 1 dependent manner. Haematologica. 2016;101(10):1216-1227.

65. Yang X, Feng W, Wang R, et al. Repolarizing heterogeneous leukemia-associated macrophages with more M1 characteristics eliminates their pro-leukemic effects. Oncoimmunology. 2018;7(4):e1412910.
66. Neering SJ, Bushnell T, Sozer S, et al. Leukemia stem cells in a genetically defined murine model of blast-crisis CML. Blood. 2007;110(7):2578-2585.
67. Li W, Li Y, Jin X, et al. CD38: A Significant Regulator of Macrophage Function. Front Oncol. 2022;12(775649.
68. Chávez-Galán L, Olleros ML, Vesin D, Garcia I. Much More than M1 and M2 Macrophages, There are also CD169+ and TCR+ Macrophages. Frontiers in Immunology. 2015;6(
69. Mussai F, De Santo C, Abu-Dayyeh I, et al. Acute myeloid leukemia creates an arginase-dependent immunosuppressive microenvironment. Blood. 2013;122(5):749-758.
70. Jablonski KA, Amici SA, Webb LM, et al. Novel Markers to Delineate Murine M1 and M2 Macrophages. PLOS ONE. 2015;10(12):e0145342.
71. Mao Z, Zhang J, Shi Y, et al. CXCL5 promotes gastric cancer metastasis by inducing epithelial-mesenchymal transition and activating neutrophils. Oncogenesis. 2020;9(7):63.
72. Kessenbrock K, Plaks V, Werb Z. Matrix metalloproteinases: regulators of the tumor microenvironment. Cell. 2010;141(1):52-67.
73. Bhattacharya A, Chowdhury A, Chaudhury K, Shukla PC. Proprotein convertase subtilisin/kexin type 9 (PCSK9): A potential multifaceted player in cancer. Biochim Biophys Acta Rev Cancer. 2021;1876(1):188581.
74. Moll NM, Ransohoff RM. CXCL12 and CXCR4 in bone marrow physiology. Expert Rev Hematol. 2010;3(3):315-322.
75. Kim M, Choi HY, Woo JW, Chung YR, Park SY. Role of CXCL10 in the progression of in situ to invasive carcinoma of the breast. Scientific Reports. 2021;11(1):18007.
76. Zhang Y, Lazarus J, Steele NG, et al. Regulatory T-cell Depletion Alters the Tumor Microenvironment and Accelerates Pancreatic Carcinogenesis. Cancer Discovery. 2020;10(3):422-439.
77. Yeh SCA, Hou J, Wu JW, et al. Quantification of bone marrow interstitial pH and calcium concentration by intravital ratiometric imaging. Nature Communications. 2022;13(1):393.

78. Stein M, Keshav S, Harris N, Gordon S. Interleukin 4 potently enhances murine macrophage mannose receptor activity: a marker of alternative immunologic macrophage activation. Journal of Experimental Medicine. 1992;176(1):287-292.
79. Doherty TM, Kastelein R, Menon S, Andrade S, Coffman RL. Modulation of murine macrophage function by IL-13. The Journal of Immunology. 1993;151(12):7151-7160.
80. Doyle AG, Herbein G, Montaner LJ, et al. Interleukin-13 alters the activation state of murine macrophages in vitro: Comparison with interleukin-4 and interferon-γ. European Journal of Immunology. 1994;24(6):1441-1445.
81. Bailey JD, Diotallevi M, Nicol T, et al. Nitric Oxide Modulates Metabolic Remodeling in Inflammatory Macrophages through TCA Cycle Regulation and Itaconate Accumulation. Cell Reports. 2019;28(1):218-230.e217.
82. Ackun-Farmmer MA, Soto CA, Lesch ML, et al. Reduction of leukemic burden via bone-targeted nanoparticle delivery of an inhibitor of C-chemokine (C-C motif) ligand 3 (CCL3) signaling. Faseb j. 2021;35(4):e21402.
83. Pinho S, Lacombe J, Hanoun M, et al. PDGFRα and CD51 mark human nestin+ sphere-forming mesenchymal stem cells capable of hematopoietic progenitor cell expansion. J Exp Med. 2013;210(7):1351-1367.
84. Morikawa S, Mabuchi Y, Kubota Y, et al. Prospective identification, isolation, and systemic transplantation of multipotent mesenchymal stem cells in murine bone marrow. J Exp Med. 2009;206(11):2483-2496.
85. Frisch BJ, Hoffman CM, Latchney SE, et al. Aged marrow macrophages expand platelet-biased hematopoietic stem cells via interleukin-1B. JCI Insight. 2019;4(10):
86. Morrison BM, Tsingalia A, Vidensky S, et al. Deficiency in monocarboxylate transporter 1 (MCT1) in mice delays regeneration of peripheral nerves following sciatic nerve crush. Exp Neurol. 2015;263(325-338.
87. Bisetto S, Whitaker-Menezes D, Wilski NA, et al. Monocarboxylate Transporter 4 (MCT4) Knockout Mice Have Attenuated 4NQO Induced Carcinogenesis; A Role for MCT4 in Driving Oral Squamous Cell Cancer. Front Oncol. 2018;8(324.
88. Benjamin D, Robay D, Hindupur SK, et al. Dual Inhibition of the Lactate Transporters MCT1 and MCT4 Is Synthetic Lethal with Metformin due to NAD+ Depletion in Cancer Cells. Cell Rep. 2018;25(11):3047-3058.e3044.

89. Sautchuk R, Eliseev RA. Cell energy metabolism and bone formation. Bone Reports. 2022;16(101594.

90. Genomic and Epigenomic Landscapes of Adult De Novo Acute Myeloid Leukemia. New England Journal of Medicine. 2013;368(22):2059-2074.

91. Bottomly D, Long N, Schultz AR, et al. Integrative analysis of drug response and clinical outcome in acute myeloid leukemia. Cancer Cell. 2022;40(8):850-864.e859.

92. Jaynes JM, Sable R, Ronzetti M, et al. Mannose receptor (CD206) activation in tumor-associated macrophages enhances adaptive and innate antitumor immune responses. Science Translational Medicine. 2020;12(530):eaax6337.

93. Xu ZJ, Gu Y, Wang CZ, et al. The M2 macrophage marker CD206: a novel prognostic indicator for acute myeloid leukemia. Oncoimmunology. 2020;9(1):1683347.

94. Su X, Xu Y, Fox GC, et al. Breast cancer-derived GM-CSF regulates arginase 1 in myeloid cells to promote an immunosuppressive microenvironment. J Clin Invest. 2021;131(20):

95. Wang J, Huang H, Lu J, et al. Tumor cells induced-M2 macrophage favors accumulation of Treg in nasopharyngeal carcinoma. Int J Clin Exp Pathol. 2017;10(8):8389-8401.

96. Sun W, Wei F-Q, Li W-J, et al. A positive-feedback loop between tumour infiltrating activated Treg cells and type 2-skewed macrophages is essential for progression of laryngeal squamous cell carcinoma. British Journal of Cancer. 2017;117(11):1631-1643.

97. Noy R, Pollard Jeffrey W. Tumor-Associated Macrophages: From Mechanisms to Therapy. Immunity. 2014;41(1):49-61.

98. Chen T, Zhou Y, Tan W-S. Influence of lactic acid on the proliferation, metabolism, and differentiation of rabbit mesenchymal stem cells. Cell Biology and Toxicology. 2009;25(6):573-586.

99. Wei L, Wei W, Qi Z, et al. Small bone marrow adipocytes predict poor prognosis in acute myeloid leukemia. Haematologica. 2018;103(1):e21-e24.

100. Saulle E, Spinello I, Quaranta MT, et al. Targeting Lactate Metabolism by Inhibiting MCT1 or MCT4 Impairs Leukemic Cell Proliferation, Induces Two Different Related Death-Pathways and Increases Chemotherapeutic Sensitivity of Acute Myeloid Leukemia Cells. Frontiers in Oncology. 2021;10(

101. Man CH, Mercier FE, Liu N, et al. Proton export alkalinizes intracellular pH and reprograms carbon metabolism to drive normal and malignant cell growth. Blood. 2022;139(4):502-522.

Tables

Table 1

Compound	t Stat	p Value	-log10(p)	FDR
lactate	5.86	2.66E-06	5.58	9.04E-05
serine	5.19	1.63E-05	4.79	0.00028
ribose-phosphate	4.37	0.00015	3.82	0.0016
citrulline	-4.29	0.00019	3.72	0.0016
DHAP	4.13	0.00029	3.54	0.0020
ornithine	3.84	0.00064	3.19	0.0037
phenylalanine	3.57	0.0013	2.88	0.0065
lysine	3.01	0.0054	2.26	0.023
glycine	2.88	0.0074	2.13	0.028

Table 1: Altered Extracellular Metabolites in Human AML Bone Marrow

Table 2

Cytokine	Reported Functions
CXCL10/IP-10	Immunosuppressive Tumor Microenvironment
LIX (CXCL5)	Tumor Growth and Metastasis
CCL12 (MCP-5)	HSC Regulation and Homing
CCL6/C10 (MRP-1)	Immunosuppressive Tumor Microenvironment
MMP3	Tumor Growth and Metastasis
Proprotein Convertase 9	Tumor Growth and Metastasis

Table 2: Cytokines Upregulated in LAM Cocultures and Reported Functions in the BM or Cancer Progression

Figure Legends

Fig. 1) Lactate is elevated in the bone marrow microenvironment (BMME) during acute myeloid leukemia (AML).

A, Graphical description of the process for metabolomic analysis of human AML vs. normal control BM extracellular fluid. **B,** Heatmap showing the relative abundance of detectable metabolites in human BM extracellular fluid of AML patients vs. controls (n = 5, in triplicates). **C,** Graphical depiction of the procedure for the generation of leukemic cells and initiation of bcCML, a murine AML model. **D,** Heatmap showing the relative abundance of detectable metabolites in murine bcCML vs. healthy BM extracellular fluid (n = 4, in triplicates). **E,** Absolute lactate concentration in AML and control human BM extracellular fluid (n = 5). **F** and **G,** Mass spectrometry (MS) peak intensity of lactate in murine (**F**) and human (**G**) BM extracellular fluid. Significance levels determined by unpaired t test for **E** is indicated as *, $P < 0.05$. Error bar indicates mean ± standard deviation (SD).

Fig. 2) Lactate contributes to the polarization of leukemia-associated macrophage (LAMs) to an alternatively activated phenotype.

A, Gating scheme for flow cytometric analysis of murine BM macrophages. **B,** Simplified Presentation of Incredibly Complex Evaluations (SPICE) analysis of LAM subpopulations from late-stage bcCML (55-70% GFP^+ cells in BM) (n = 5), red arrows indicate populations lost and black arrow indicate populations enriched in disease. **C** and **D,** Frequency of $CD206^{hi}$ (**C**) and mean fluorescence intensity (MFI) of CD206 on $CD206^+$ (**D**) non-leukemic control macrophages (Ctrl), leukemia-associated macrophages (LAMs), or leukemic (GFP^+) macrophages (n = 7). **E-F,** Bulk RNA sequencing of LAMs vs. macrophages from nonleukemic (NL) controls: heatmap of differentially expressed genes (**E**) and principal component analysis (PCA) of the top 500 variable genes (**F**). **G,** Cytokine profiling by ELISA of cell culture supernatant from NL macrophages or LAMs cocultured on a BM stromal monolayer (n = 2), representative example, arrows shown indicating a qualitative difference. **H** and **I,** Bone marrow-derived macrophage (BMDM) expression of CD206, polarized *in vitro* by treatment with 10 mmol/L lactate, lipopolysaccharide (LPS) as proinflammatory stimuli, and/or IL-4 and IL-13 as suppressive stimuli, in serum-free media for 12 hours (**H**) (n = 6) or 1 week (**I**) (n = 3). **J,** Range of relative quantification (RQ) of Arginase 1 (*Arg1*) transcripts in BMDMs polarized by lactate (L) and/or

IL-4 and -13 (ILs), measured by RT-qPCR (n = 3, in duplicates). Significance levels determined by one-way ANOVA for **C, D, H,** and **I** are indicated as: *, $P < 0.05$; **, $P < 0.01$; ***, $P < 0.001$; ****, $P < 0.0001$. Error bar indicates mean ± SD.

Fig. 3) Lactate drives loss of hematopoietic stem and progenitor cell (HSPC) function and support.

A, Experimental procedure to assay for HSPC hematopoietic colony-forming potential, by colony-forming unit cell (CFU-C) assays: Murine HSPCs/LSKs are cocultured with a BM stromal monolayer and 60,000 added macrophages. **B,** CFU-Cs after coculture with LAMs or nonleukemic control (Ctrl) macrophages (n = 4). **C,** CFU-C of HSPCs alone, with or without added lactate for 48 hours (**C**) (n = 4). **D-E,** CFU-C assays of HSPCs and stromal monolayer cocultures for 72 hours with or without added lactate: CFU-Cs relative to the 0 mmol/L lactate control group (**D**) (n = 12-14) and graphic of experimental procedure (**E**). **F-H,** BM MSC differentiation to osteoblasts (OBs) with or without lactate treatment: relative area of colony-forming unit pre-osteoblastic (CFU-preOB) colonies visualized with alkaline phosphatase staining at day 14 (**F**) (n = 6), relative area of calcium deposition measured by silver nitrate staining at day 28 (**G**) (n = 6), representative image of Pre-OB colonies (**H**). **I-K,** Lactate treatment of MSCs grown in a non-differentiation culture media: representative image of colony-forming unit fibroblasts (CFU-F) (**I**) and relative number of colonies on day 10 (**J**) (n = 6), relative cell number of whole BM MSCs by day 14 (**K**) (n = 6). Significance levels determined by unpaired t test for **B** and by one-way ANOVA for **C**, **F-G**, and **J-K** are indicated as: *, $P < 0.05$; **, $P < 0.01$; ***, $P < 0.001$; ****, $P < 0.0001$. Error bar indicates mean ± SD.

Fig. 4) GPR81 drives leukemia-associated macrophage (LAM) polarization.

A, Graphical depiction of the procedure for the initiation of wt bcCML in a *Gpr81*$^{-/-}$ BMME **B,** Frequency of macrophages, out of live non-leukemic (GFP^{-}) cells, from the BM of wt bcCML initiated in wt or *Gpr81*$^{-/-}$ (GPR81KO) mice, relative to nonleukemic (NL) controls of the same genetic background (n = 4-7). **C-E,** Marker expression on BM LAMs of wt bcCML initiated in wt or *Gpr81*$^{-/-}$ (GPR81KO) mice, or NL controls: Frequency of CD206^{+} macrophages in the BM (**C**), expression of CD206 on CD206^{+} BM macrophages relative to relative to NL controls of the same genetic background (**D**), frequency of MHCII^{+} BM macrophages (**E**) (n = 4-11). **F,** MFI of

CD206 on CD206^{+} wt or *Gpr81*$^{-/-}$ BMDMs polarized by LPS, IL-4 and -13 (ILs), and/or 10 mmol/L lactate (n = 3). **G,** Frequency of CD206^{hi} wt or GPR81$^{-/-}$ BMDMs with or without polarization by ILs and lactate. **H,** Range of relative quantification (RQ) of *Arg1* expression by wt or GPR81KO BMDMs polarized by IL-4 and -13 (ILs) with or without lactate, measured by RT-qPCR (n = 3, in duplicates). Significance levels determined by one-way ANOVA for **B-G** are indicated as: ns, not significant; *, $P < 0.05$; **, $P < 0.01$; ***, $P < 0.001$; ****, $P < 0.0001$. Error bar indicates mean ± SD.

Fig. 5) GPR81 signaling partially regulates HSPC function.

A-F, Hematopoietic progenitors' frequency in the BM of wt bcCML initiated in wt or GPR81KO mice, relative to the nonleukemic (NL) control of the same genetic background: hematopoietic stem and progenitor cells (HSPCs/LSK) (**A**), long-term hematopoietic stem cell (HSC) (**B**), short-term HSC (**C**), multipotent progenitor (MPP) subsets MPP2 (**D**) MPP3 (**E**) and MPP4 (**F**) (n = 4). **G-I,** Mesenchymal stem cell (MSC) populations in bone: MSCs (**G**), PααV MSCs (**H**), and PαS MSCs (**I**) (n = 4). **J-K,** CFU-Cs of wt or *Gpr81*$^{-/-}$ (G^{-}) lactate-treated HSPCs alone (**J**) or with a stromal monolayer (**K**), relative to 0 mmol/L lactate (n = 4-8). **L-M,** CFU-preOB (**L**) and CFU-F (**M**) of wt or *Gpr81*$^{-/-}$ MSCs with lactate treatment, relative to the 0 mmol/L lactate control of the same genetic background. Significance levels determined by one-way ANOVA for all are indicated as: ns, not significant; *, $P < 0.05$; **, $P < 0.01$; ***, $P < 0.001$; ****, $P < 0.0001$. Error bar indicates mean ± SD.

Fig. 6) GPR81 signaling is a driver of leukemia cell growth and leukemia stem cell (LSC) self-renewal.

A, Graphical depiction of the procedure for the initiation of *Gpr81*$^{-/-}$ (GPR81KO) bcCML cells in wt or GPR81KO mice (GPR81 DKO). **B-D,** Leukemic burden in the bone marrow (BM) (**B**), peripheral blood (**C**), and spleen (**D**), of wt or GPR81KO bcCML initiated in wt mice, by the timepoint of wt late-stage disease (n = 5). **E-G,** Leukemic burden in the BM (**E**), peripheral blood (**F**), and spleen (**G**) at the time of wt bcCML early-stage disease, initiated using wt or GPR81KO bcCML cells in wt or GPR81KO mice (n = 4). **H,** Leukemic burden in the BM over time of wt or GPR81KO bcCML (n = 5-7). **I,** Time to progression to late-stage disease in wt or GPR81 DKO bcCML (n = 5). **J-K,** LSC repopulation assays of wt vs. *Gpr81*$^{-/-}$ bcCML cells: number of colonies

at each passage (**J**)**,** and probability of survival by passage (**K**) (n = 3, in duplicates). Significance levels determined by one-way ANOVA for **B-G,** unpaired t tests for **H**, and log-rank (Mantel-Cox) test for **I** and **K**, are indicated as: ns, not significant; *, $P < 0.05$; **, $P < 0.01$; ***, $P < 0.001$; ****, $P < 0.0001$. Error bar indicates mean ± SD.

Fig. 1)

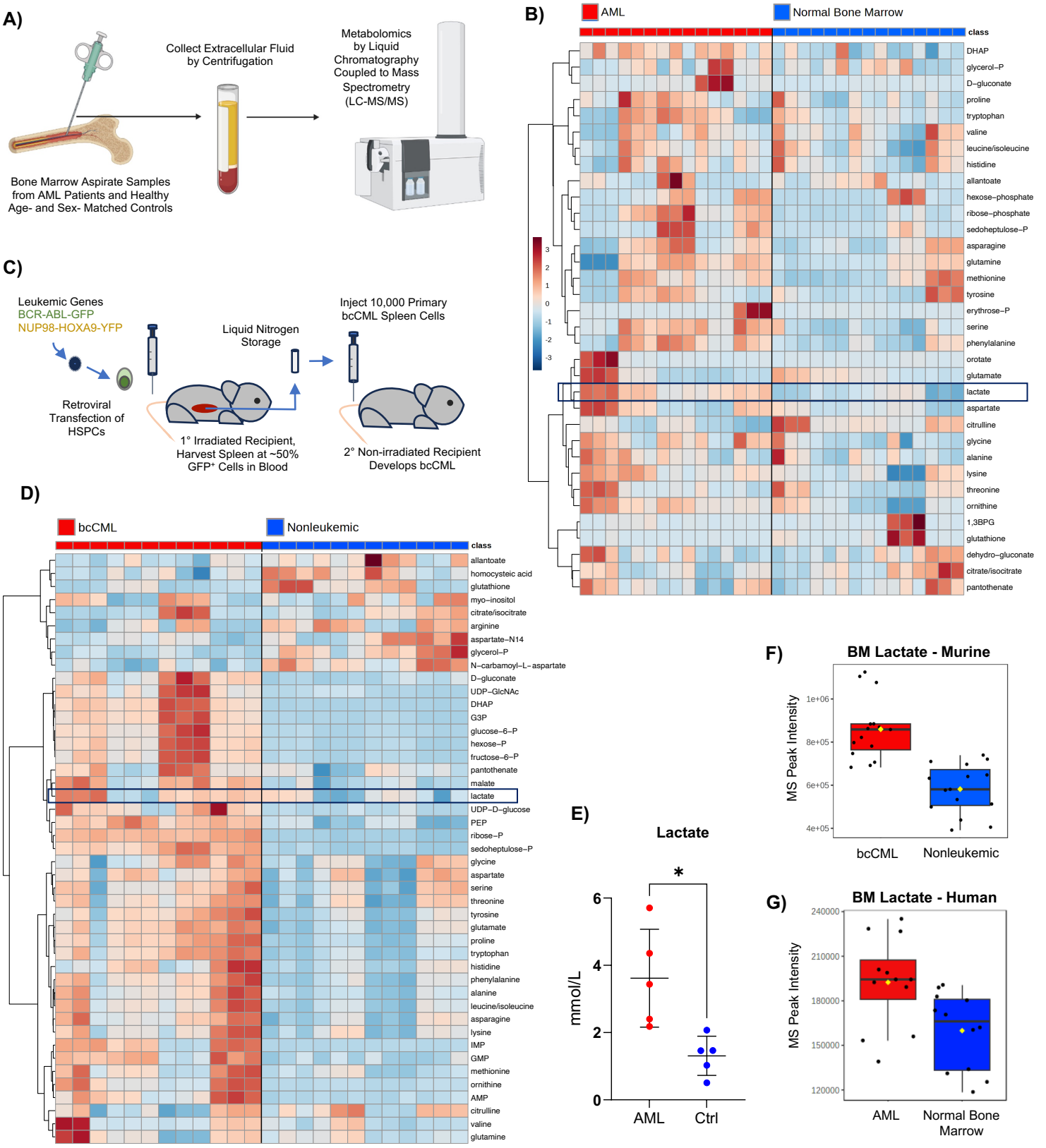
A)
Collect Extracellular Fluid by Centrifugation
Metabolomics by Liquid Chromatography Coupled to Mass Spectrometry (LC-MS/MS)
Bone Marrow Aspirate Samples from AML Patients and Healthy Age- and Sex- Matched Controls
B)
AML
Normal Bone Marrow
class
DHAP
glycerol−P
D−gluconate
proline
tryptophan
valine
leucine/isoleucine
histidine
allantoate
hexose−phosphate
ribose−phosphate
sedoheptulose−P
asparagine
glutamine
methionine
tyrosine
erythrose−P
serine
phenylalanine
orotate
glutamate
lactate
aspartate
citrulline
glycine
alanine
lysine
threonine
ornithine
1,3BPG
glutathione
dehydro−gluconate
citrate/isocitrate
pantothenate
C)
Leukemic Genes
BCR-ABL-GFP
NUP98-HOXA9-YFP
Retroviral Transfection of HSPCs
Liquid Nitrogen Storage
1° Irradiated Recipient, Harvest Spleen at ~50% GFP⁺ Cells in Blood
Inject 10,000 Primary bcCML Spleen Cells
2° Non-irradiated Recipient Develops bcCML
D)
bcCML
Nonleukemic
class
allantoate
homocysteic acid
glutathione
myo−inositol
citrate/isocitrate
arginine
aspartate−N14
glycerol−P
N−carbamoyl−L−aspartate
D−gluconate
UDP−GlcNAc
DHAP
G3P
glucose−6−P
hexose−P
fructose−6−P
pantothenate
malate
lactate
UDP−D−glucose
PEP
ribose−P
sedoheptulose−P
glycine
aspartate
serine
threonine
tyrosine
glutamate
proline
tryptophan
histidine
phenylalanine
alanine
leucine/isoleucine
asparagine
lysine
IMP
GMP
methionine
ornithine
AMP
citrulline
valine
glutamine
E)
Lactate
mmol/L
AML
Ctrl
F)
BM Lactate - Murine
MS Peak Intensity
bcCML
Nonleukemic
G)
BM Lactate - Human
MS Peak Intensity
AML
Normal Bone Marrow

Fig. 2)

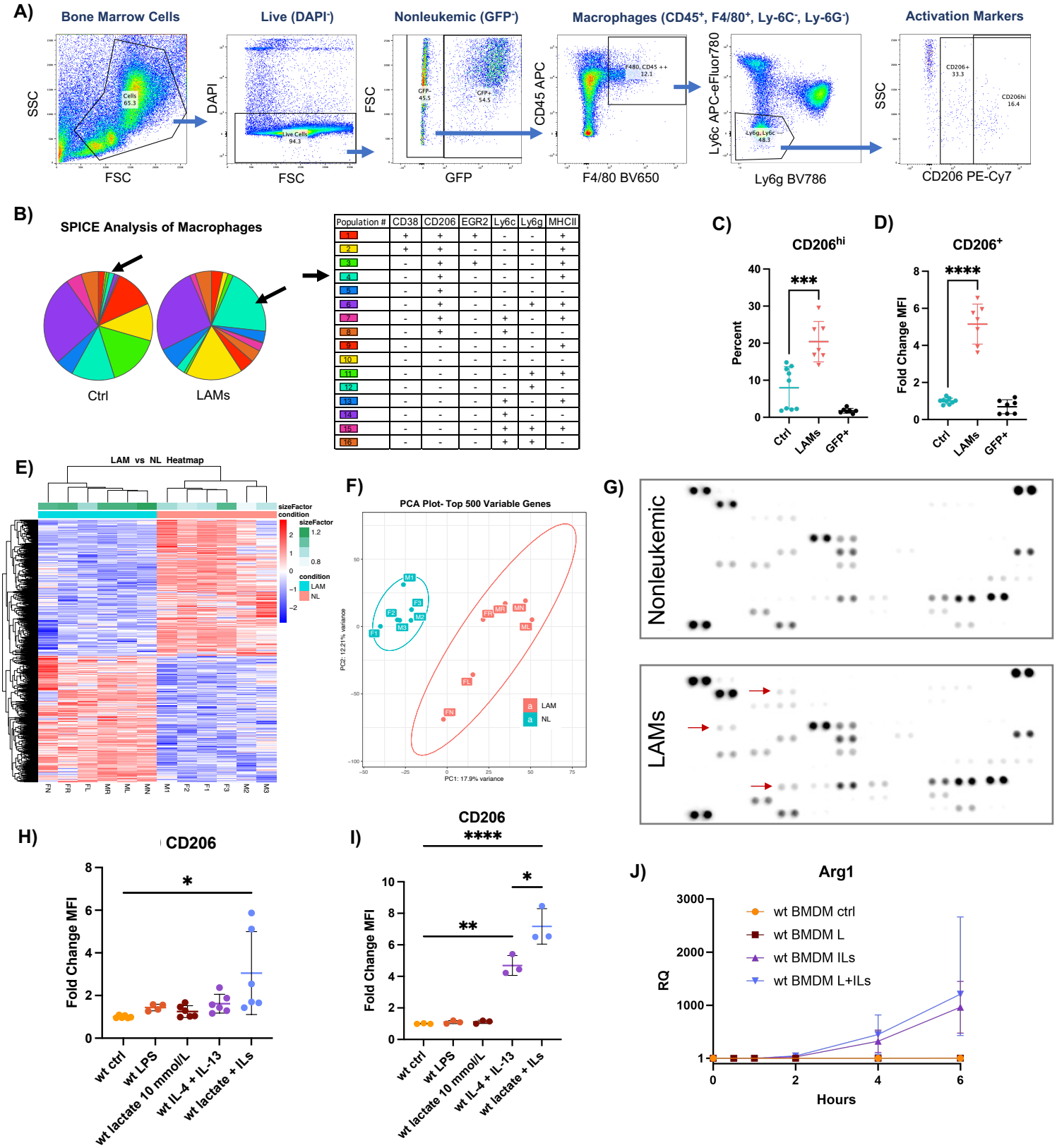

Population #	CD38	CD206	EGR2	Ly6c	Ly6g	MHCII
1	+	+	+	-	-	+
2	+	+	-	-	-	+
3	-	+	+	-	-	+
4	-	+	-	-	-	+
5	-	+	-	-	-	-
6	-	+	-	-	+	+
7	-	+	-	+	-	+
8	-	+	-	+	-	-
9	-	-	-	-	-	+
10	-	-	-	-	-	-
11	-	-	-	-	+	+
12	-	-	-	-	+	-
13	-	-	-	+	-	+
14	-	-	-	+	-	-
15	-	-	-	+	+	+
16	-	-	-	+	+	-

Fig. 3)

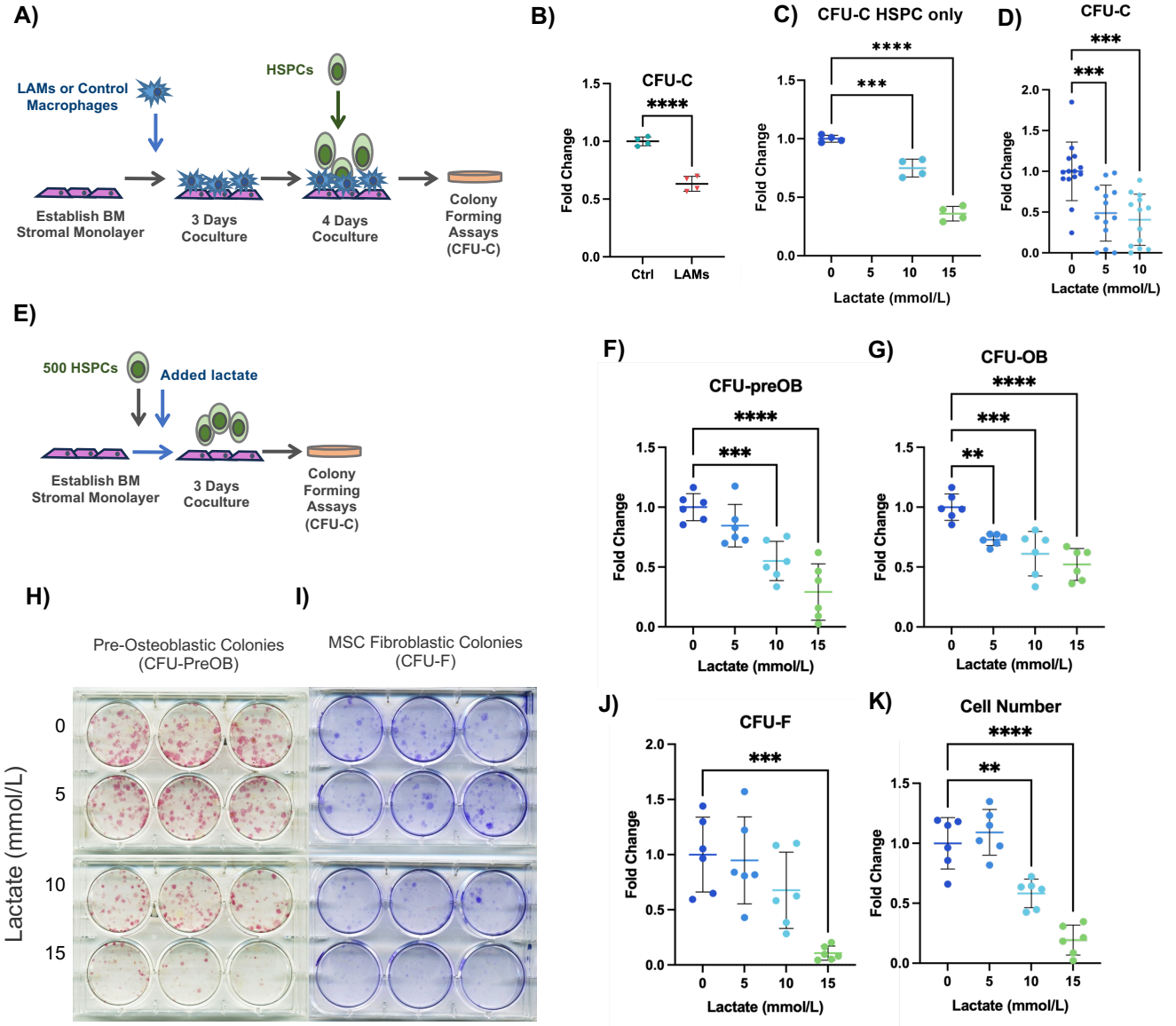
A)
LAMs or Control Macrophages
HSPCs
Establish BM Stromal Monolayer
3 Days Coculture
4 Days Coculture
Colony Forming Assays (CFU-C)
B)
CFU-C
****
Fold Change
Ctrl
LAMs
C)
CFU-C HSPC only
****
***
Fold Change
Lactate (mmol/L)
D)
CFU-C
***
***
Fold Change
Lactate (mmol/L)
E)
500 HSPCs
Added lactate
Establish BM Stromal Monolayer
3 Days Coculture
Colony Forming Assays (CFU-C)
F)
CFU-preOB
****
***
Fold Change
Lactate (mmol/L)
G)
CFU-OB
****
***
**
Fold Change
Lactate (mmol/L)
H)
Pre-Osteoblastic Colonies (CFU-PreOB)
I)
MSC Fibroblastic Colonies (CFU-F)
Lactate (mmol/L)
0
5
10
15
J)
CFU-F
***
Fold Change
Lactate (mmol/L)
K)
Cell Number
****
**
Fold Change
Lactate (mmol/L)

Fig. 4)

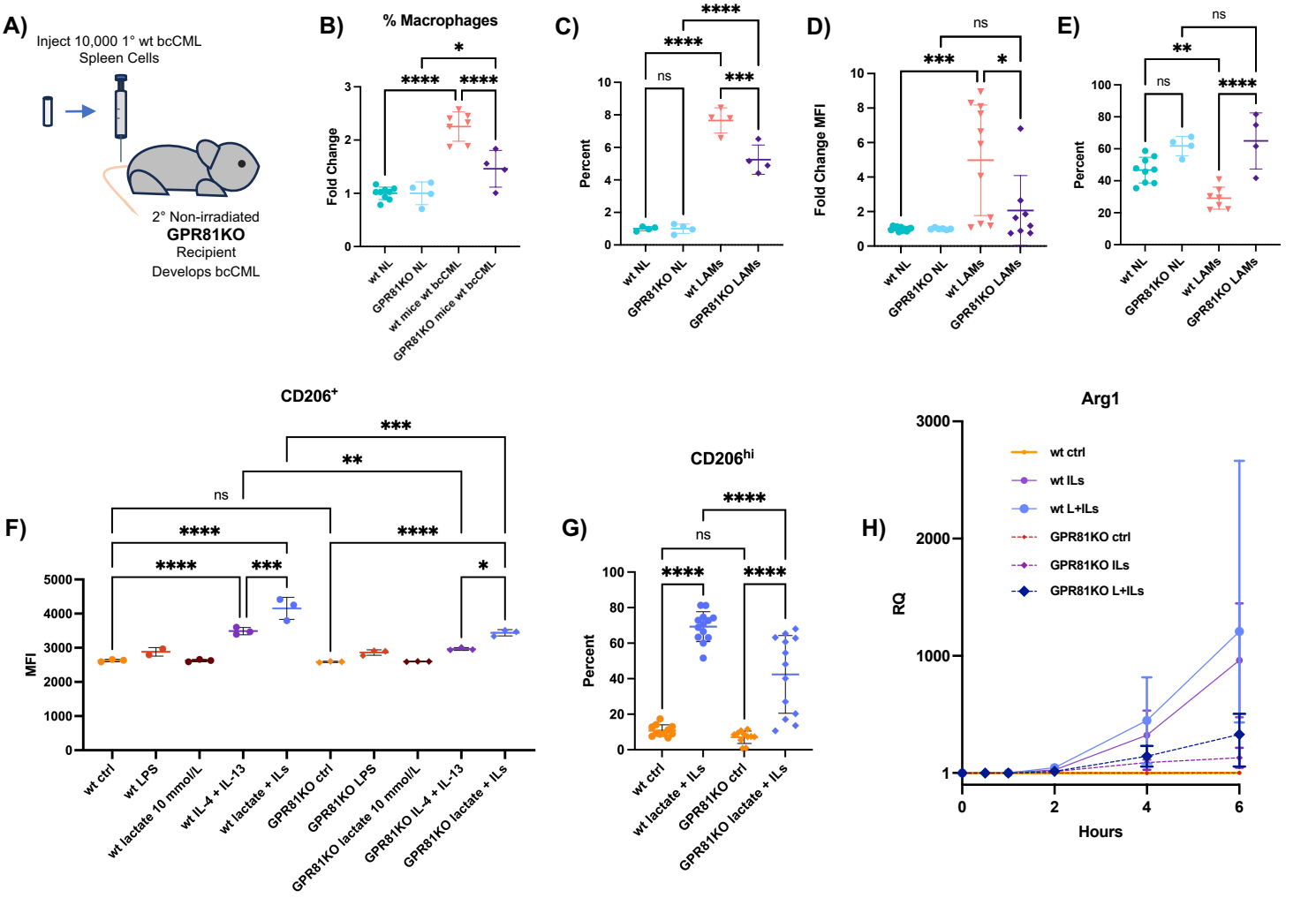
A)
Inject 10,000 1° wt bcCML
Spleen Cells
2° Non-irradiated
GPR81KO
Recipient
Develops bcCML
B)
% Macrophages
Fold Change
wt NL
GPR81KO NL
wt mice wt bcCML
GPR81KO mice wt bcCML
C)
CD206+
Percent
wt NL
GPR81KO NL
wt LAMs
GPR81KO LAMs
D)
CD206+
Fold Change MFI
E)
MHCII+
Percent
F)
CD206+
MFI
wt ctrl
wt LPS
wt lactate 10 mmol/L
wt IL-4 + IL-13
wt lactate + ILs
GPR81KO ctrl
GPR81KO LPS
GPR81KO lactate 10 mmol/L
GPR81KO IL-4 + IL-13
GPR81KO lactate + ILs
G)
CD206hi
Percent
H)
Arg1
RQ
Hours
wt ctrl
wt ILs
wt L+ILs
GPR81KO ctrl
GPR81KO ILs
GPR81KO L+ILs

Fig. 5)

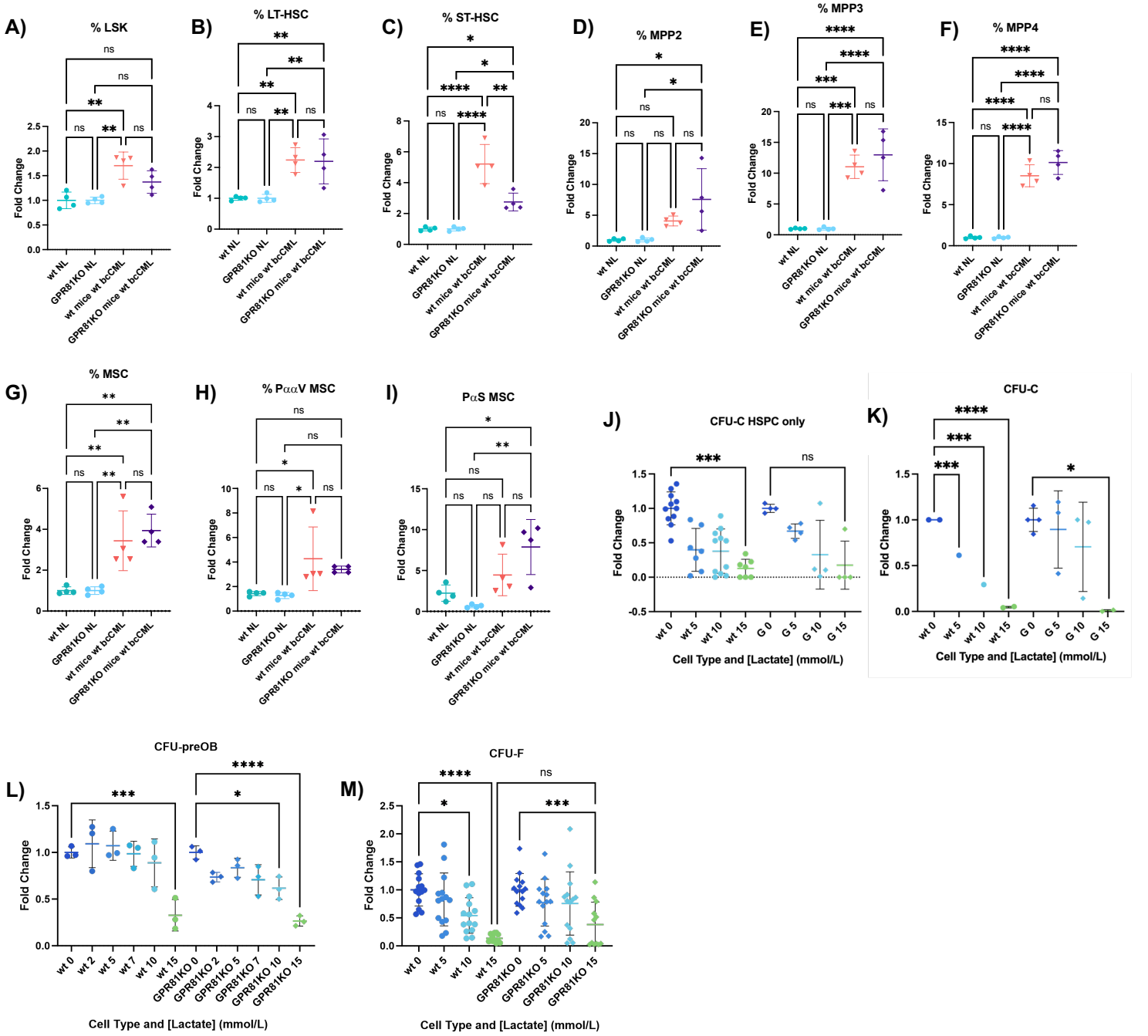
A)
% LSK
B)
% LT-HSC
C)
% ST-HSC
D)
% MPP2
E)
% MPP3
F)
% MPP4
G)
% MSC
H)
% PααV MSC
I)
PαS MSC
J)
CFU-C HSPC only
K)
CFU-C
L)
CFU-preOB
M)
CFU-F
Fold Change
wt NL
GPR81KO NL
wt mice wt bcCML
GPR81KO mice wt bcCML
Cell Type and [Lactate] (mmol/L)

Fig. 6)

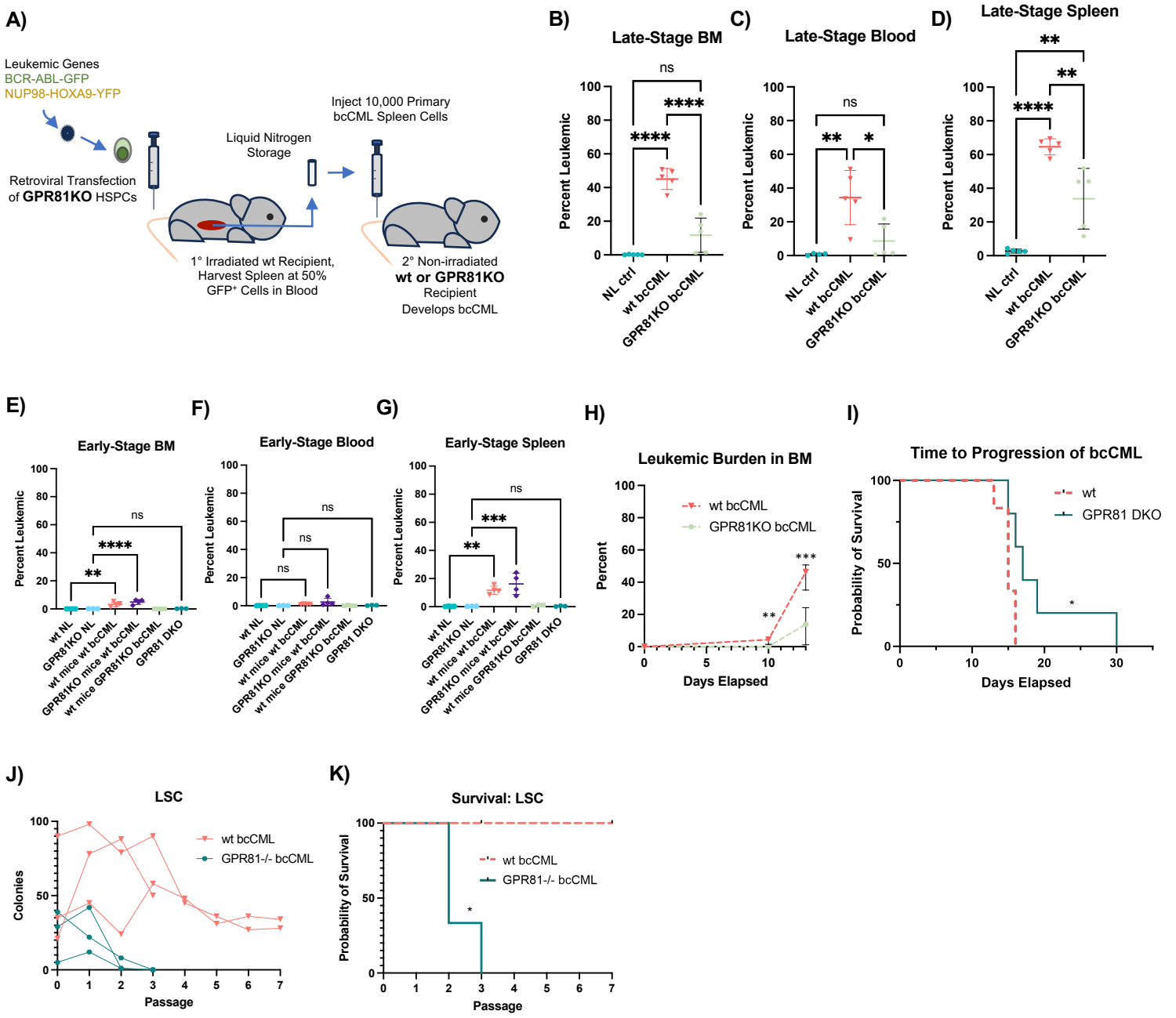
A)
Leukemic Genes
BCR-ABL-GFP
NUP98-HOXA9-YFP
Retroviral Transfection of GPR81KO HSPCs
Liquid Nitrogen Storage
Inject 10,000 Primary bcCML Spleen Cells
1° Irradiated wt Recipient, Harvest Spleen at 50% GFP+ Cells in Blood
2° Non-irradiated wt or GPR81KO Recipient Develops bcCML
B)
Late-Stage BM
C)
Late-Stage Blood
D)
Late-Stage Spleen
Percent Leukemic
NL ctrl
wt bcCML
GPR81KO bcCML
ns
****
**
*
E)
Early-Stage BM
F)
Early-Stage Blood
G)
Early-Stage Spleen
wt NL
GPR81KO NL
wt mice wt bcCML
GPR81KO mice wt bcCML
wt mice GPR81KO bcCML
GPR81 DKO
***
H)
Leukemic Burden in BM
Percent
Days Elapsed
I)
Time to Progression of bcCML
Probability of Survival
wt
GPR81 DKO
J)
LSC
Colonies
Passage
wt bcCML
GPR81-/- bcCML
K)
Survival: LSC